Desalination and Water Treatment
www.deswater.com

doi:10.5004/dwt.2016.11100

61 (2017) 160–169
January

Preliminary evaluation of the use of vacuum membrane distillation for the production of drinking water in Arica (Chile)

Juan A. Andrés-Mañas[a], Patricia Palenzuela[a,*], Lorena Cornejo[b], Diego C. Alarcón-Padilla[a], Gabriel Acién[c], Guillermo Zaragoza[a]

[a]*CIEMAT-Plataforma Solar de Almería, Ctra. de Senés s/n, 04200 Tabernas, Almería, Spain*
Tel. +34 950387800 Ext. 909, Fax +34 950365015, email: patricia.palenzuela@psa.es
[b]*Laboratorio de Investigaciones Medioambientales de Zonas Áridas, LIMZA, Escuela Universitaria de Ingeniería Mecánica, EUDIM, Universidad de Tarapacá, Arica, Chile*
[c]*Department of Chemical Engineering, University of Almería, 04120 Almería, Spain*

Received 9 June 2015; Accepted 7 June 2016

ABSTRACT

In the context of a national Chilean project, a pilot membrane distillation (MD) plant built by Aquaver using a novel configuration of vacuum multi-effect membrane distillation (V-MEMD) patented by memsys will be implemented in a rural area of Arica (northern Chile) called Cuya. The nominal production of the plant is 60 l h^{-1} and the heat is supplied with a hybrid system composed of a solar field and a diesel generator (i.e. its waste heat), working alternatively according to the solar radiation availability. The aim of this paper is to assess the feasibility of the system for supplying drinking water to the population. A prediction of the performance of the desalination system based on a similar unit has been used together with a typical meteorological year in order to dimension the solar field required. The simulations show that drinking water needs can be fully covered on a yearly basis using a field of stationary solar thermal collectors with a total area of 70.5 m^2, to generate about 49% of the total heat required for a 24 h d^{-1} operation. The diesel generator can supply waste heat to cover the rest of the thermal energy demand, as well as an electricity production which can decrease the producing cost of water to about 1.2 $ m^{-3}.

Keywords: Solar thermal desalination; Membrane distillation; Vacuum multi-effect membrane distillation; Modelling and simulation

1. Introduction

Supply and demand for fresh water have increased gradually in the last two decades. Sustainable growth of human activities is thus becoming increasingly more difficult since water is totally necessary for these activities. These circumstances together with the fact that most of places with fresh water scarcity are located close to the sea make the use of desalination processes for obtaining fresh water of vital importance for these places. The water scarcity problem is even worse in rural and isolated areas due to the lack of territorial policies and a continuous and appropriate supply of energy. These facts make almost impossible the development of suitable infrastructures for obtaining potable water in these regions, which would suppose an economic push for the improvement of their main activities (farm, fishing, etc.). Desalination in these areas, which are characterized by a low fresh water demand (less than 20 m^3 d^{-1}), requires decentralized systems able to work efficiently for obtaining water with full guarantees of quality and healthiness. These systems must also be simple in order to be handled and maintained by non-very-qualified staff without frequent

*Corresponding author.

Presented at EuroMed 2015: Desalination for Clean Water and Energy Palermo, Italy, 10–14 May 2015. Organized by the European Desalination Society.

stops. In this sense, renewable-energy-driven desalination technologies satisfy all these requirements to produce water with suitable quality in these areas.

Northern Chile is one of the most arid regions in the world. It is placed in the solar belt, and therefore it receives a big amount of solar radiation per year. Pollution of natural water with several dangerous contaminants from the volcanic activity, such as arsenic, is another added problem in this region. Arsenic levels are in the range of 1.0–1.3 mg l^{-1} [1], which can lead to irreversible damages in the medium term in the central nervous system and diverse kinds of cancer. The Chilean government has become aware of this serious problem and since early 90's plans and regulations based on ISO14001 are being developed, for standardizing lucrative activities that do not be friendly with the environment. The need of obtaining drinking water from this contaminated source, and the high availability of solar radiation, constitute an appropriate scenario for the installation of robust solar desalination techniques. In this context, membrane distillation (MD) driven by solar energy is presented as a promising technology to satisfy the potable water requirements in isolated areas of northern Chile.

Membrane distillation is a novel thermal desalination process fully implementable at low and medium scale in remote places when the demand is less than 20 m^3 d^{-1}. It is a relatively new non-isothermal process known since the late 1960's, although it did not receive too much interest until the early 1980's, when better membranes and modules were developed, with lower costs. The availability of new commercial microporous membranes (made in different materials and with specific morphologies and structures) has allowed more research in this area, in terms of increasing the productivity and the energy efficiency of the distillation process [2]. MD systems have advantages like relative low cost, simplicity and modularity. As opposed to the industrial thermal desalination techniques, MD can be implemented in batch mode, which allows its use in places without high demand of freshwater. Furthermore, the possibility of using waste heat or renewable energies for the heat supply makes MD an especially interesting thermal separation process [3].

MD is driven by a partial pressure gradient of water vapour between both sides of the membrane, not by the absolute pressure as in other membrane processes like reverse osmosis [2]. Membranes, commonly made of polymers like polypropylene (PP), polytetrafluoroethylene (PTFE), or polyvinylidene fluoride (PVDF) have pore sizes between 0.1 and 1 μm, must have low thermal conductivity for avoiding excessive heat losses, low surface energy and high surface tension for the feed solution, in order to increasing the liquid entry pressure and avoiding pore wetting. The rejection of ions and non-volatiles in the mix is almost total. The development of MD has brought about different configurations of the technology. One of the most promising nowadays is vacuum membrane distillation (VMD). It is a useful technique for separating volatile compounds from aqueous solutions [4]. The removal of air from the permeate side of the system using vacuum pressure lower than the equilibrium vapour pressure of water, permits the reduction of heat losses by conduction and the increasing of the transmembrane flux. Lab-scale experiments have been carried out with good agreement with theoretical predictions [2,5,6]. The great amount of thermal energy needed in the process is the major drawback of this desalination process. Several studies have been focused on the application of different renewable energies or the use of waste heat as energy source for heating the feed going into the VMD system [7,8]. Moreover, memsys is developing since 2010 an innovative multi-effect VMD (V-MEMD) device for improving the energy efficiency of VMD processes. It allows recovering the latent heat from one stage to the next, reducing the energy required in the process. In each stage, vapour phase goes across the membrane and condenses on a foil, delivering its latent heat to the feed in the next stage. Due to the evaporation process, the feed increases its salinity while circulating from one stage to another (Fig. 1). Memsys modules have a high development potential due to the low specific heat transfer surface, high water flux, low heat loss, internal heat recovery by evaporation and condensation, minimum mechanical stress in the membranes, and flexible and modular construction [9]. In addition, it is important to highlight the potential of this innovative device to treat more concentrated sources without a significant loss of the system performance [10].

As in conventional VMD, V-MEMD has been tested with renewable and fossil energy sources. A V-MEMD unit

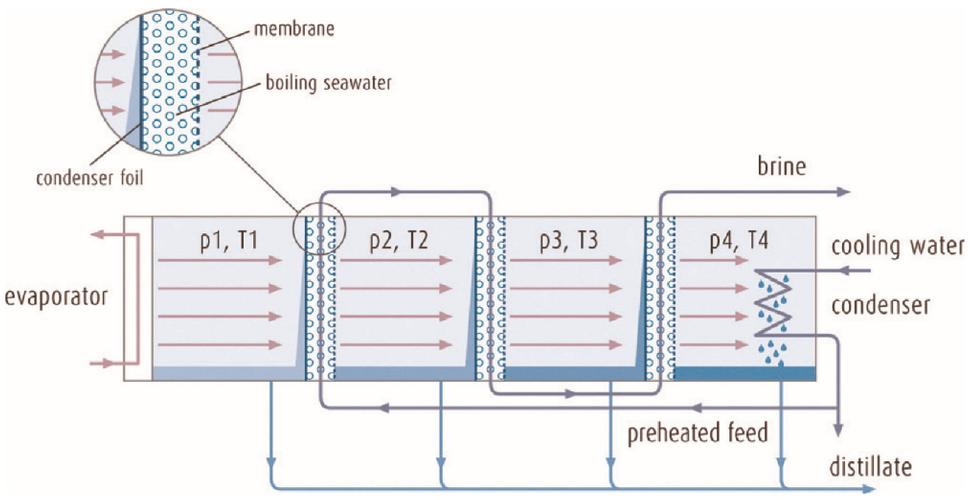

Fig. 1. Diagram showing the movement of brine and distillate in a V-MEMD unit (from [9]).

driven by solar energy has been evaluated at the Plataforma Solar de Almería using simulated seawater as the feed source [11]. Concentration factors of 2.5 (similar to those of reverse osmosis) were obtained as well as a reduction in the conductivity of the feed up to 4 orders of magnitude. The plant required specific thermal energy consumption below 400 kWh_{th} m^{-3}. Experiments using a diesel heater have been also reported by Zhao et al. [3]. It was observed that the energy efficiency is not strongly influenced by the change in the feed flow rate. Higher distillate fluxes were obtained at higher feed flow rates, but also higher energy consumptions were required. The use of more effects in the MD plant provided more heat recovery and therefore lower thermal energy consumption, but with more capital costs [12]. The innovative concept of memsys has been also put into practice in remote places, such the Maldives Islands, using the waste heat from a diesel generator. An economic evaluation of the system proved a large reduction in the maintenance and energy costs per cubic meter comparing with the same operation using a reverse osmosis plant [8].

In this work, a commercial V-MEMD system (called MDS-40B) has been evaluated for drinking water production considering its coupling with a hybrid solar-waste heat source. It has been built by the company Aquaver, and bears a memsys module. The desalination plant will be placed at Cuya, Arica (Chile), a volcanic Andean region located at 116 km far from Arica that counts with a surface of 955 km^2 and 142 inhabitants. An autonomous photovoltaic (PV) solar field (2 kWp) will be installed for obtaining the necessary electricity for internal consumption into the desalination plant. Thermal energy will be obtained from a solar thermal field and from the cooling circuit of a diesel generator when the solar radiation availability is not enough. Considering the temperature range that MD works, low temperature solar thermal collectors are the most suitable, and within this classification, flat-plate collectors have been selected for the projected solar field. The electricity from the diesel generator will be supplied to the nearby community.

The size of the solar field required for providing the thermal energy to the V-MEMD plant has been firstly determined. Secondly, the annual solar contribution to the total energy use has been evaluated. For this purpose, an annual simulation of the solar field has been run and the annual solar fraction (which is the relation between the amount of energy obtained through the solar technology used and the total annual energy required by the process) has been determined. Finally, the annual fresh water produced from the different energy supply systems has been calculated, and the monthly variation of the solar fraction analysed.

2. Membrane distillation system

The system MDS-40B (Fig. 2) has a module with a steam raiser (SR), four stages, and a condenser (C). The total membrane area is 6.4 m^2. As it has been described previously, module components are made of PP and membranes of PTFE, with a mean pore diameter of about 0.2 µm. Condensation foils are also made of PP and have a thickness of 40 µm [9]. Because of the nature of the membranes, the feed water temperature is limited to 80ºC [13]. Before entering the module, the feed water is pre-filtered using a cartridge filter with mean pore diameter of 40 µm. Then, it is used in the condenser and part of the pre-heated feed is introduced in the steam raiser. This is an innovation of the Aquaver integration regarding standard memsys operation as depicted in Fig. 1, where a closed circuit of distilled water is used in the steam raiser and the feed enters in the first stage. An external energy source is used only in the steam raiser, where the feed water boils at a reduced temperature due to the vacuum generated inside the module. Here, the first vapour is produced, which passes through the membrane and condenses onto a foil when delivering its latent heat to the feed water flowing through the next stage. Notice that the feed water that leaves each stage at a certain temperature (called brine) evaporates by flashing when entering the following one as the stage is at a lower pressure. Then, the brine generates vapour until it achieves the equilibrium temperature corresponding to the pressure in the stage. Therefore, the decrease in the brine temperature is high enough to condensate the vapour that

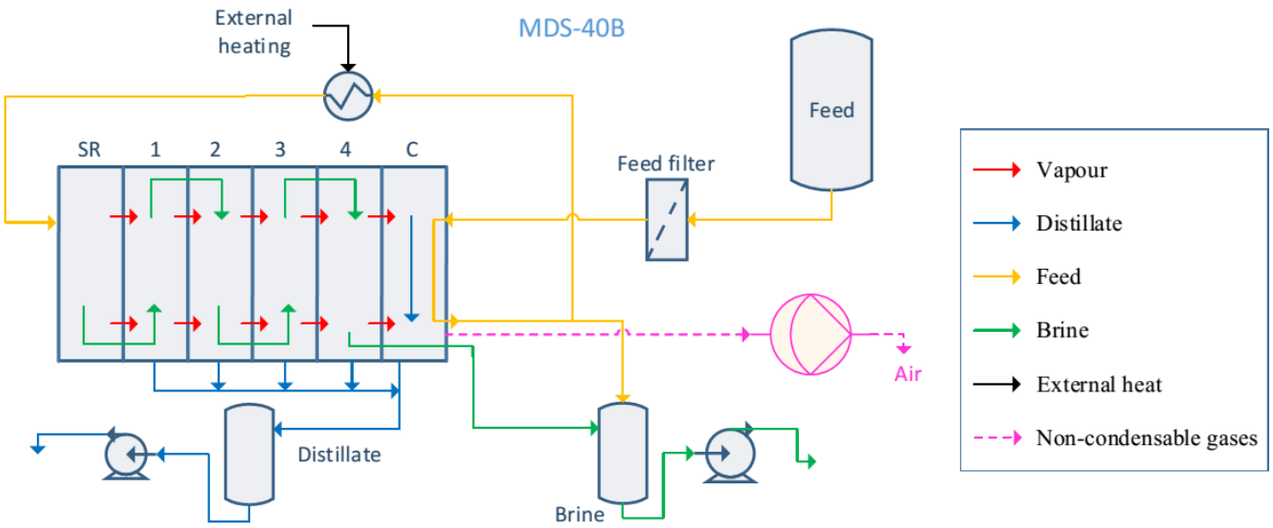

Fig. 2. Diagram for the MDS-40B system.

comes from the previous stage. Likewise, the latent heat of condensation is transferred to this brine to be further evaporated. The same process is repeated in all the stages, part of the brine is evaporated (being more concentrated in salts) firstly by flash and then by the thermal energy transferred by the vapour generated in the previous stage, and vapour is condensed producing distillate. Such distillate water is extracted from each stage. The vapour produced in the final stage is condensed using feed water as cooling medium. Part of this water is rejected together with the brine helping to dilute it before its disposal, and the other part is the preheated feed water that goes into the module, as is the case in other thermal desalination processes like multi-stage flash and multi-effect distillation [14]. The resulting products are on one side, an almost pure water (with a very low conductivity), and, on the other side, concentrated brine that is sent back to the feed water source.

The MDS-40B unit requires a maximum thermal power of 14 kW_{th} for its operation in nominal conditions. This thermal energy could be supplied with either the solar thermal field or waste heat from an electric generator, which works with diesel fuel. Figs. 3 and 4 show an evaluation of the system in terms of water production and energy efficiency, respectively, using a theoretical model developed by Aquaver [15]. Feed water temperatures at the outlet of the heat exchanger (T_{ths}) of 60, 70, and 80°C were simulated, with flow rates of 1.5, 2.0, and 2.5 l min^{-1}. Vacuum pressure and feed water temperature at the inlet of the condenser were set to 60 mbar and 20°C, respectively, for all case simulations. A plate-and-frame exchanger with 13 plates and area of 0.451 m^2 was considered to provide the heat needed in the MD system. Fig. 3 shows the distillate flux (distillate production per unit of membrane area) simulated for the different operating conditions. A correlation between the thermal power and the distillate flux has been obtained from the mentioned figure: $y = 1.06\,x - 3.17$, being "y" the distillate flux [l h^{-1} m^{-2}], and "x" the thermal power supplied [kW_{th}], with $R^2 = 0.9584$. As expected, the higher the thermal power supplied to the feedwater in the heat exchanger, the bigger the distillate production is. As shown in Fig. 3, higher values of thermal power supply increase the feedwater temperature in the heat exchanger, causing an increase in the distillate flux. The effect of changing the feedwater flow rate is less pronounced. As

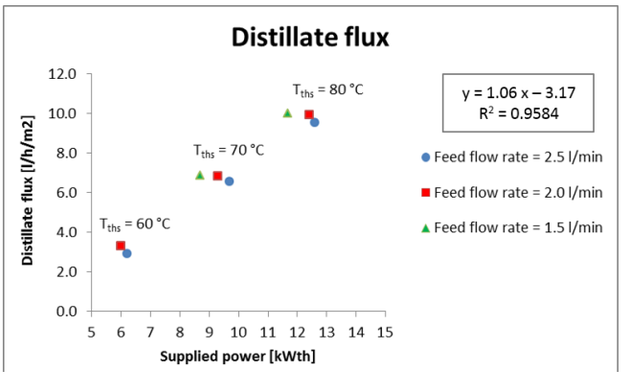

Fig. 3. Theoretical results for the influence of supplied thermal power in the distillate flux.

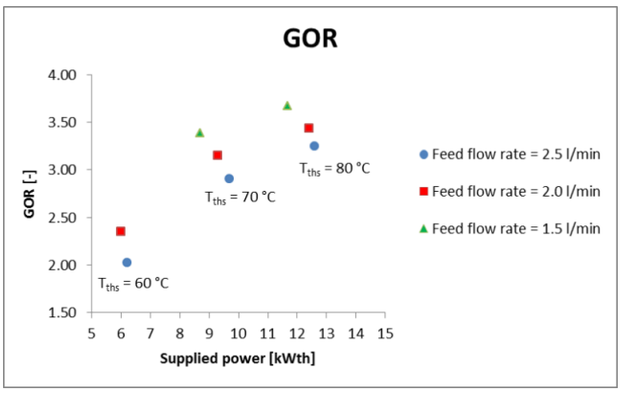

Fig. 4. Theoretical results for the influence of supplied thermal power in the GOR.

can be observed, a rise in the feedwater temperature from 60 to 80°C (related to an increase by a factor of 2 in the thermal consumption) resulted in a three times higher distillate production.

Fig. 4 shows the variation of the thermal efficiency of the desalination plant with the supplied power at different feed flow rates. The efficiency is commonly represented by a parameter called Gain Output Ratio (GOR), which is the ratio between the latent heat used to produce the total amount of distillate, and the total heat supplied to the system. A GOR equal to 1 means that all the energy supplied to the system is used to produce distillate. The maximum theoretical value of GOR in a multi-effect system based on latent heat recovery coincides with its number of effects, four in this case. Considering the heat losses in a real system, memsys established a rule of thumb for GOR estimation in their modules as 0.78 times the number of effects [13].

Fig. 4 shows that, as in the case of the distillate flux, an increase in the thermal power supplied to the system produces an increase in the GOR values, not with a linear trend in this case, but approaching asymptotically to the maximum value discussed before. For a constant value of the feed flow rate, the increase of the GOR with an increase in the feedwater temperature from 60 to 70°C is much larger than from 70 to 80°C. For the same feedwater temperature, there is an increase in the GOR when the feed flow rate decreases. It is because the decrease in the thermal power supplied by the reduction in the feedwater flow rate is higher than the decline in the distillate production (Fig. 3), which makes GOR to increase.

3. Design and simulation of the energy system

3.1. Solar field

The selection of the solar collector technology has been based on the temperature range of operation of the MD plant and the meteorological conditions of Cuya, Arica (Chile). From the many types of solar collectors available, these three merit further consideration for their application to MD plants: the compound parabolic collector (CPC), the evacuated tube collector (ETC), and the flat-plate collector

(FPC). Their efficiency is usually represented as a function of the mean temperature of the collector (T_{col}) (average between the inlet and outlet temperatures of the heat transfer fluid inside the collector) and the ambient temperature (T_{amb}). ETC collectors have higher efficiency for larger values of ($T_{col} - T_{amb}$). However, they have two main disadvantages: higher capital costs and lower durability due to the time that the vacuum can be maintained inside the tubes of the collectors (roughly between 7 to 10 y), which makes their maintenance costs much higher. The FPCs operate with a high efficiency at low values of ($T_{col} - T_{amb}$). However, when ($T_{col} - T_{amb}$) increases, the efficiency of these collectors decreases drastically.

CPC collectors show a similar behaviour as the FPCs, but their overall efficiency is lower. Since the expected T_{amb} in Cuya, Arica (Chile) is not very high, FPCs could be a good option for the required T_{col} values of about 85ºC.Therefore, FPC collectors have been selected to provide the thermal energy needed in the MD plant. Table 1 shows the technical characteristics (aperture area and flow rate) of the chosen collectors along with the efficiency parameters: incident angle modifier ($K_{\tau\alpha}$), optical efficiency (η_{opt}) and the coefficients accounting for thermal losses (c_1 and c_2) as provided by the manufacturers.

The collectors are orientated to the North and with a tilt angle equal to the local latitude. As mentioned above, the location of the solar MD plant is Cuya, Arica (Chile) with the following geographical coordinates: lat. 19.20°S, long. 70.28°W. The solar field has been dimensioned for a specific design point (specific date, including month, day and time), which has been selected at the 18th of June at solar noon (this time corresponds to sun zenith and presents greater stability of the direct solar irradiation) in order to have an annual solar contribution close to 50%. The irradiation and ambient temperature data of the selected location have been taken from a typical meteorological year (TMY) generated with Meteonorm® software (see in Table 2 the monthly data of global irradiation over tilted plane and ambient temperature) and they have been normalized with the actual measurement of the yearly global irradiation over tilted plane (G–G_K, 2110 kWh m^{-2} y^{-1}) obtained from a radiometric measuring solar station located close to the selected location.

Firstly, the design of the solar field has been carried out by determining the number of collectors in series in a row and the number of rows in parallel, and then a yearly simulation of the solar field has been performed in order to determine the thermal power and the solar fraction

Table 1
Technical specifications and efficiency parameters of the commercial static solar collectors selected for this study

Eurotherm ESK 2.5 SB	
Aperture area (A_a): 2.35 m^2	
$K_{\tau\alpha}$(50º): 0.94	
Efficiency parameters	η_{opt}: 0.766
	c_1: 4.52 W K^{-1} m^{-2}
	c_2: 0.0042 W K^{-2} m^{-2}
Flow rate: 0.014 kg s^{-1} m^{-2}	

Table 2
Data of irradiation and ambient temperature of a TMY in Cuya, Arica

Month	G–G_K [kWh m^{-2}]	T_{amb} [ºC]
January	188	22.1
February	180	22.4
March	205	22.1
April	141	20.0
May	105	18.3
June	92	17.3
July	86	17.0
August	86	16.6
September	111	16.1
October	144	17.1
November	157	18.2
December	194	20.3

provided. The number of collectors in series in a row is determined by the ratio between the temperature increase required in a row and the temperature step of an individual solar collector. This has been established taking into account the operational temperature of the feedwater in the V-MEMD plant, which has been set to 80ºC. Assuming a 5ºC temperature difference in the heat exchanger located between the thermal source and the V-MEMD plant (Fig. 5), the minimum temperature of the hot water at the outlet of the solar field results to be 85ºC. A water temperature difference between the inlet and outlet of the solar field of 10ºC has been considered, thus the temperature increase in the solar field has been fixed from 75 to 85ºC. Then, the temperature step of a static collector is determined from Eq. (1) that represents the efficiency of the collector η_i:

$$\eta_i = \frac{\dot{m}\cdot C_p\cdot(T_{out} - T_{in})}{G_k\cdot A_a} = \eta_{opt}\cdot K_{\tau\alpha} - c_1\cdot\left[\frac{(T_{col} - T_{amb})}{G_K}\right] - c_2\cdot\left[\frac{(T_{col} - T_{amb})^2}{G_K}\right] \quad (1)$$

where $\dot{m}$ is the heat transfer fluid (i.e. water) mass flow rate through the solar collector; C_p is the average heat capacity of the heat transfer fluid; T_{col} is the average between the inlet and outlet temperatures of the collector; T_{in} and T_{out} are the inlet and outlet temperatures in the solar collector, respectively; G_k is the global solar irradiance on tilted plane in W m^{-2}; A_a is the aperture area of the collector; c_1, c_2 and η_{opt} are the efficiency parameters of the collector, and $K_{\tau\alpha}$ is the incident angle modifier (Table 1). This latter parameter is determined at any incidence angle using Eq. (2), which is valid only for FPCs:

$$K_{\tau\alpha} = 1 - b_o\left(\frac{1}{\cos\theta} - 1\right) \quad (2)$$

where b_o is a constant parameter called coefficient of the incident angle modifier and θ is the incident angle (that is calculated as the arc cosine of the dot product between the normal vector to the collector aperture plane and the solar vector).

From the previous equation T_{out} is determined assuming T_{in} as the average between the inlet and outlet temperatures in the solar field. On the other hand, the number of solar field rows connected in parallel is calculated as the ratio between the thermal power to be supplied by the solar field (that is the thermal power required by the MD process at nominal conditions, 14 kW_{th}, considering a solar multiple of 1) and the thermal power supplied by one individual row. This last one is determined from the thermal power supplied by one collector (according to Eq. (1)), multiplied by the number of collectors connected in series.

Once the solar field was dimensioned, an annual simulation of its performance was run. The solar field computer model was developed by the authors based on the thermal losses of the collectors, their efficiency curve and energy balances, and it was implemented using MATLAB programming language. The simulation procedure consists in assuming firstly an initial inlet temperature to the solar field close to the ambient temperature, then in determining the outlet temperature of each collector and therefore of the row (or from the solar field) from Eq. (1). With the outlet temperature and considering an initial flow rate equal to that one given in the technical specifications of the collector, the thermal power provided by each row and therefore by the solar field is determined. A loop determines the outlet temperature from the solar field in each time interval and recalculates the flow rate in cases in which the outlet temperature from the solar field is lower than that established to be reached (85ºC). As explained above, meteorological data given by the software Meteonorm® have been used for the yearly simulation. These data have been taken in intervals of 1 h for every day of the year. From the yearly simulation, the thermal energy provided by the solar field during the year (sum of the thermal power provided in each interval multiplied by the time interval) can be determined and with this and with the total annual energy required by the process the solar fraction is calculated. The same procedure is used for the monthly solar fraction but considering the meteorological data of each month.

3.2. Diesel generator

When solar heat is not enough for maintaining the fresh water demand, heat from the cooling circuit of a diesel generator is supplied to the desalination module. The projected diesel generator has been built by the Dutch company Bredenoord, customized for the use of its waste heat. It has an output of 15 kVA and works at 1500 rpm with cos ψ = 0.8, at 230 or 400 V. The thermal power that the generator can provide to the desalination system is 13 kW_{th}. The generator is connected to a heat accumulator and provides the heat to the MDS-40B desalination system (Fig. 5). In order to avoid a lack of cooling in the generator, a regulation valve detects if there is a not-very-high heat consumption in MDS-40B, and in this case, switches automatically to the original cooling circuit.

4. Integrated V-MEMD solar field diesel generator

The overall desalination system to be implemented consists of the previously discussed elements (Fig. 5): the MD module MDS-40B, the solar field (thermal and PV), the

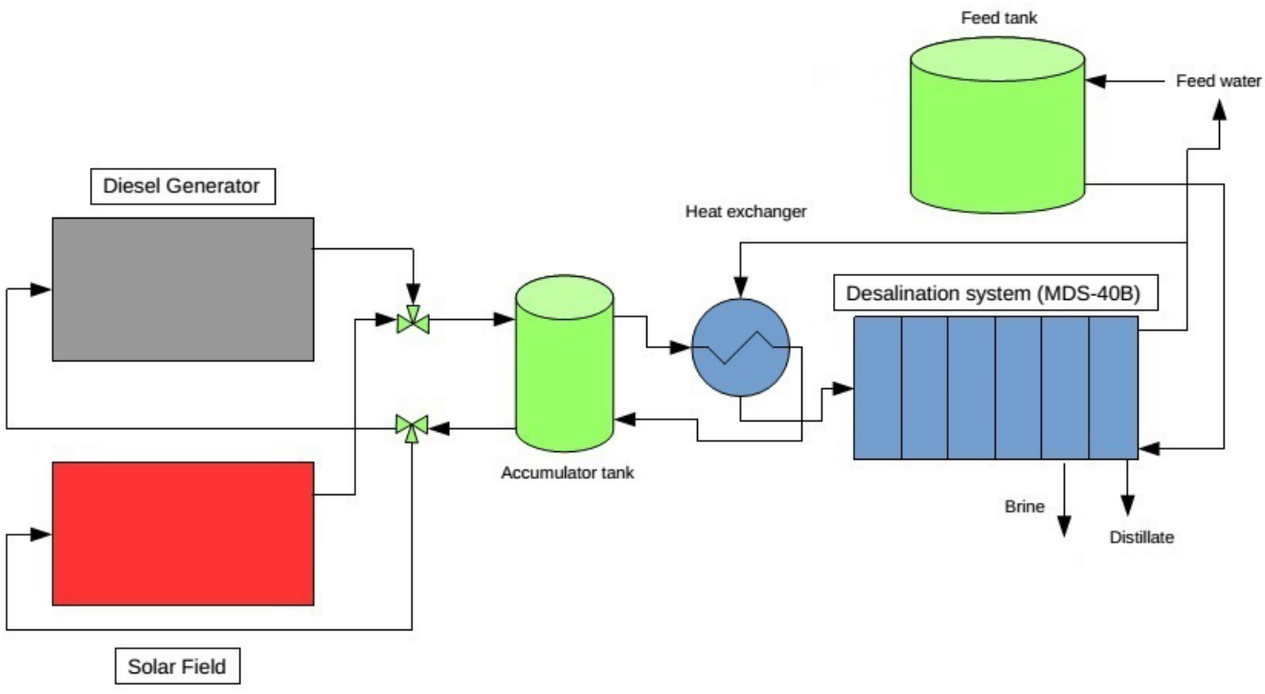

Fig. 5. Diagram for the desalination unit at Cuya, Arica.

Table 3
Solar field dimensioning results: outlet temperature of the collector (T_{out}), thermal power supplied by one collector (P_{col_fluid}), number of collectors in series in one row (N_{col_series}), number of rows in parallel (N_{rows}), total number of collectors (N_{total}) and total aperture area (A_T)

Variables	Values
T_{out}	83.21 °C
P_{col_fluid}	0.44 kW_{th}
N_{col_series}	3
N_{rows}	10
N_{total}	30
A_T	70.5 m^2

diesel generator, a heat accumulator, and a feed tank. The combination will operate as a whole, synchronized depending on the amount of heat needed to cover the fresh water demand. The default operating option will use the heat produced in the solar field. In this operation mode, the diesel generator will be kept switched off, and the autonomous PV field will provide the plant with the required electricity. In absence of enough solar radiation for the nominal heat that covers the fresh water demand, the diesel generator will turn on, and a 3-way regulation valve will change the cooling circuit. In this situation, water from the accumulator tank will be the cooling liquid for the generator, and electricity produced by the diesel generator will be supplied to the community (strengthening their commercial activity). Depending on the energy produced by the solar field (solar heat), as will be shown in the following section, the percentage of usage of the diesel generator will be higher or lower. On the other hand, the autonomous PV field will be providing the electricity required by the MD unit. In this manner, there will be always electricity for the desalination plant and enough heat in the membrane module to obtain the required distillate production, which will be free of contaminants, including arsenic.

5. Results and discussion

The results of the projected solar thermal field for the selected design point are shown in Table 3. Solar field is formed by 30 flat-plate collectors, arranged in 10 rows of 3 collectors each. Water circulates in reversed return, in order to maintain a uniform feed flow rate in each row. The total aperture area is 70.5 m^2, and the outlet temperature from a solar collector is 83.21°C. The thermal power delivered by one solar collector to the fluid is 0.44 kW_{th}.

Fig. 6 shows the variation of the thermal power provided by the solar collectors along the year in Cuya.

Fig. 7 represents the solar fraction obtained every month. As it can be observed, the solar fraction obtained in summer months is almost three times that of the winter months. The annual average solar fraction is 49% (represented in Fig. 7 by a dotted line), which is exceeded from November to April, so half the year. According to the meteorological data, March is the month with the highest solar fraction, 78%, and from December to March the solar fraction is above 66%. In October, solar fraction is very close to the average, while in winter months, from June to August, it is up to 25% lower, which implies a more extensive use of waste heat from the diesel generator. The annual energy provided by the solar field is 6×10^4 $kWh_{th.}$

The correlation presented before (obtained using the data in Fig. 3), has been utilised to calculate the monthly fresh water production as a function of the thermal power delivered by the solar field. The results of the monthly fresh water production with solar energy along the year are presented in Fig. 8.

UNESCO establishes the minimum needs of potable water in 5 l per person and day, which means an average of 21.6 m^3 per month taking the population of Cuya. This

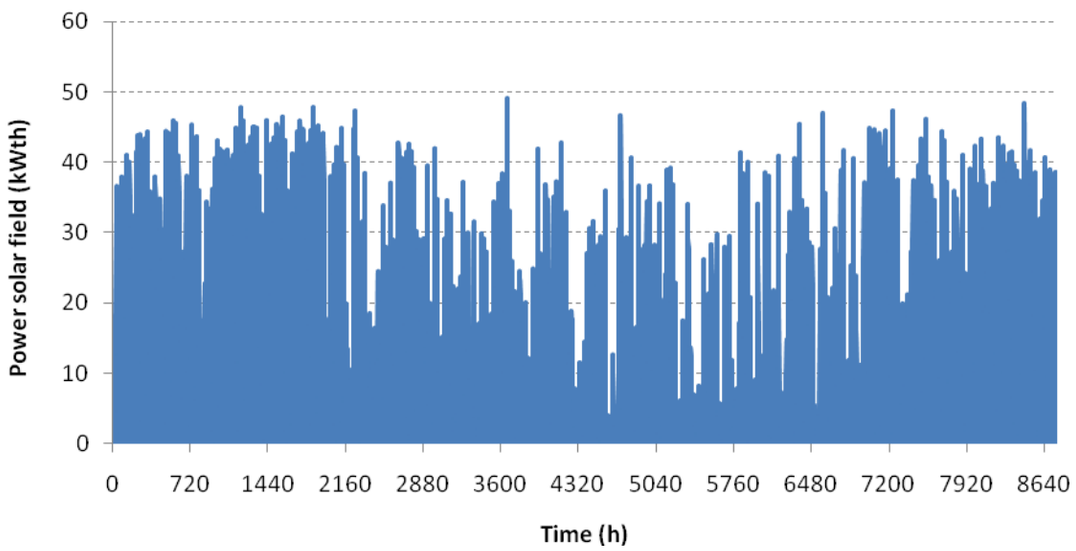

Fig. 6. Variation of the thermal power along the year with the solar field of Cuya, Arica.

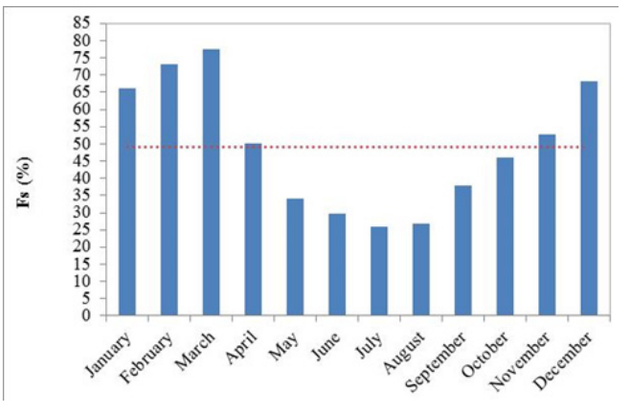

Fig. 7. Monthly solar fraction in Cuya, Arica (blue bars) and annual average solar fraction (red dotted line).

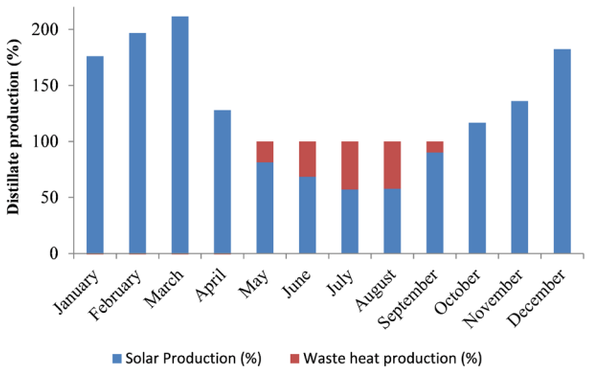

Fig. 9. Relative distillate production with respect the potable water demand established by UNESCO, using solar thermal energy (blue bars) and using waste heat (red bars) along the year.

organization also fixes a minimum requirement of 25 l per person and day for domestic and hygienic use, besides the drinking water.

A better representation of the relative figures is found in Fig. 9. It shows the ratio between the monthly distillate produced by solar energy and the monthly fresh water demanded (the amount of potable water established by UNESCO) (blue bars) and the same ratio but with the monthly distillate produced by the waste heat from the diesel generator (red bars). As expected, the percentage of the monthly distillate production by solar energy falls radically at the beginning of autumn and rises from September onwards, following the same trend as the solar fraction. Because of that, the distillate produced by the waste heat from the diesel generator is bigger in July and August for covering the 100% of the potable water demand in this period.

It can be observed that the freshwater production obtained using the solar field covers the needs of drinking water established by UNESCO most of the year. Only from May to September the waste heat has to be used partially, especially the months of June, July, and August. During these months, 32, 43 and 42%, respectively, of the minimum drinking water required will be produced by the waste heat from the diesel generator. In May, 20% will also be covered by waste heat and in September only 10%. Due to the fact that the amount of fresh water produced from November to April exceeds the 100% of the minimum needs, this surplus can be used to cover the remaining parts of the year when the solar radiation is not enough.

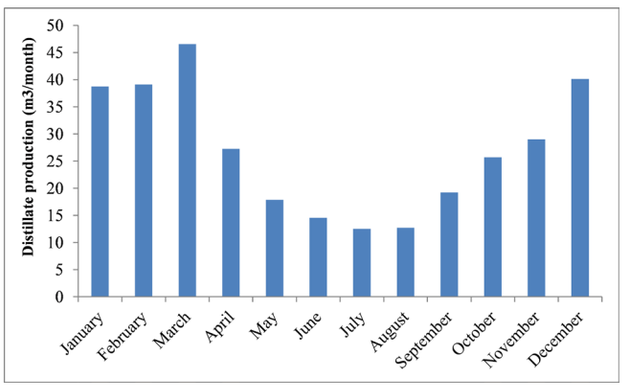

Fig. 8. Monthly solar distillate production in Cuya, Arica.

On the other hand, according to the theoretical simulations shown in Fig. 3, values of distillate flux around 10 l h^{-1} m^{-2} can be obtained working at nominal conditions (feed temperature of 80ºC, feed flow rate of 2.5 l min^{-1}) regardless the thermal energy source. Regarding the thermal energy efficiency of the module in such conditions, values of GOR around 3.25 are expected. This value is also in agreement with the estimations made by memsys, based on the number of stages in the module.

Since the technology is not commercially deployed yet, the economics have been analysed by performing a rough estimation of the water production cost *COW* ($ m^{-3}), given by Eq. (3):

$$COW = \frac{K_{CC} - K_{rev}}{PW_T} \tag{3}$$

where: K_{CC} is the yearly capital cost ($ $year^{-1}$), $K_{CC} = \frac{K_{invest}}{n} + K_{O\&M}$, being K_{invest} the investment cost ($), n the amortization time (years) and $K_{O\&M}$ the Operation and Maintenance cost ($ $year^{-1}$); PW_T is the amount of water produced per year (m^3 y^{-1}) and K_{rev} the revenues from selling the electricity ($ $year^{-1}$).

For calculating the yearly capital cost, the following investment costs have been considered: 400 $ m^{-2} for the solar thermal installation (including storage), 2 $ Wp^{-1} for the PV system, and 18,000 $ for the diesel generator, assuming an amortization period of 20 y in all cases. For the desalination unit an investment cost of 22,000 $ has been considered, and an amortization time of 5 y for the module (which takes up around 8% of the investment cost in this small unit) and 10 y for the rest of the system. O&M costs have been estimated as 5% the yearly capital cost, adding the fuel cost of the generator which has been calculated considering a 1 $ l^{-1} price of diesel and a ratio of 40 litres of diesel consumed per litre of distillate produced. Finally, a yearly production of 525.6 m^3 of water has been taken into account, and a selling price

for the electricity of 136 c$ kWh^{-1} (average of industrial and commercial electricity price in Chile [16]), being the total electricity production 67014 kWh y^{-1}. The resulting cost of distilled water is 1.2 $ m^{-3}. This cost estimation is affected by the economy of scale, since the installation is small. Costs are expected to decrease if the installation is larger, especially regarding the MD system.

6. Conclusions

V-MEMD is a novel thermal desalination technique suitable for being installed in remote regions with few population and low water demand, such as rural zones in Arica, Chile. A desalination system made by memsys and Aquaver and called MDS-40B has been simulated along a whole year using an annual model of the solar field and a theoretical correlation of the distillate production with the thermal energy supply. Using meteorological data from Arica, a thermal solar field has been dimensioned for supplying the nominal thermal power of 14 kW_{th} to the MDS-40B unit. 30 flat-plate collectors are projected, with total aperture area of 70.5 m^2. The internal electricity requirements are also guaranteed by a PV field and the use of the diesel generator as an auxiliary system, making the whole system completely autonomous. The waste heat of a diesel generator will be used when the solar radiation is not available to supply the thermal power required to produce the fresh water demanded with the aim of 24 h d^{-1} operation.

Using a typical meteorological year, an annual solar fraction of 49% has been obtained. The simulation gives a total amount of fresh water produced in the plant of 525.6 m^3 y^{-1}, 61.5% of which is obtained exclusively with solar thermal energy. An average volume of 10.1 l d^{-1} can be provided to each inhabitant of Cuya. Regarding only the drinking water needs, they can be fully covered during most of the year by the solar field, having some months (from October to April) with a surplus of fresh water that could be used to cover the remaining parts in the months when the solar fraction is not so high. Therefore, the system seems viable to supply the drinking water needs for the population of Cuya.

Acknowledgements

This work has been partially funded by project FIC Cod. BIP 30170173-0 financed by the Regional Government of Arica and Parinacota (Chile) and the Solar Energy Research Center (SERC-CHILE, CONICYT - FONDAP 15110019).

Symbols and abbreviations

A	—	Area [m^2]
b0	—	Constant for coefficient K [–]
c	—	Efficiency parameter [W K^{-N} m^{-2}]
C	—	Condenser, Specific heat [J kg^{-1} $^oC^{-1}$]
COW	—	Water production cost [$ m^{-3}]
CPC	—	Compound Parabolic Collector [–]
ETC	—	Evacuated Tube Collector [–]
FPC	—	Flat-Plate Collector [–]
G	—	Global irradiation [Wh m^{-2}]
GOR	—	Gain Output Ratio [–]
K	—	Modifier parameter; Cost [$, $ y^{-1}]
$\dot{m}$	—	Heat transfer fluid mass flow rate [kg s^{-1}]
MD	—	Membrane distillation
n	—	Amortization period [y]
N	—	Number
P	—	Power [W]
PP	—	Polypropylene
PTFE	—	Polytetrafluoroethylene
PV	—	Photovoltaic
PVDF	—	Polyvinylidene fluoride
PWT	—	Produced water [m^3 y^{-1}]
SR	—	Steam raiser
T	—	Temperature [^oC]
TMY	—	Typical meteorological year
VMD	—	Vacuum membrane distillation
V-MEMD	—	Vacuum multi-effect membrane distillation

Greek

α	—	Absorbance
η	—	Efficiency
θ	—	Incident angle [^{o}]
τ	—	Transmittance
ψ	—	Phase angle in alternate current [^{o}]

Subscripts

a	—	Aperture
amb	—	Ambient
cc	—	Capital
col	—	Collector
col_fluid	—	Collector fluid
col_series	—	Collectors in series
i	—	Collector number
in	—	Inlet
invest	—	Investment
K	—	Tilted plane
opt	—	Optical
out	—	Outlet
O&M	—	Operation & Maintenance
p	—	Constant pressure
rev	—	Revenues
T	—	Total
th	—	Thermal

References

[1] L. Cornejo, H. Lienqueo, M. Arenas, J. Acarapi, D. Contreras, J. Yáñez, H.D. Mansilla, In field arsenic removal from natural water by zero-valent iron assisted by solar radiation, Environ. Pollut., 156 (2008) 827–831.

[2] M. Khayet, Membranes and theoretical modeling of membrane distillation: a review, Adv. Colloid Interf, Sci., 164 (2011) 56–88.

[3] K. Zhao, W. Heinzl, M. Wenzel, S. Büttner, F. Bollen, G. Lange, S. Heinzl, N. Sarda, Experimental study of the memsys vacuum-multi-effect-membrane-distillation (V-MEMD) module, Desalination, 323 (2013) 150–160.

[4] K.W. Lawson, D.R. Lloyd, Membrane distillation, J. Membr. Sci., 124 (1997) 1–25.

[5] A. Alkhudhiri, N. Darwish, N. Hilal, Membrane distillation: a comprehensive review, Desalination, 287 (2012) 2–18.
[6] M. Abd El-Rady Abu-Zeid, Y. Zhang, H. Dong, L. Zhang, H. Chen, L. Hou, A comprehensive review of vacuum membrane distillation technique, Desalination, 356 (2015) 1–14.
[7] J.P. Mericq, S. Laborie, C. Cabassud, Evaluation of systems coupling vacuum membrane distillation and solar energy for seawater desalination, Chem. Eng. J., 166 (2011) 596–606.
[8] Operating data from memsys installation shows energy-positive desalination, Membr. Technol., 9 (2014) 8.
[9] W. Heinzl, S. Büttner, G. Lange, Industrialized modules for MED desalination with polymer surfaces, Desal. Wat. Treat., 42 (2012) 177–180.
[10] G. Naidu, Y. Choi, S. Jeong, T.M. Hwang, S. Vigneswaran, Experiments and modelling of a vacuum membrane distillation for high saline water, J. Indust. Eng. Chem., 20 (2014) 2174–2183.
[11] G. Zaragoza, A. Ruiz-Aguirre, E. Guillén-Burrieza, Efficiency in the use of solar thermal energy of small membrane desalination systems for decentralized water production, Appl. Energy, 130 (2014) 491–499.
[12] Y. Zhang, Y. Peng, S. Ji, Z. Li, P. Chen, Review of thermal efficiency and heat recycling in membrane distillation processes, Desalination, 367 (2015) 223–239.
[13] memDist 4-6.4, Technical description of process, modules and applications, memsys datasheets.
[14] P. Palenzuela, A.S. Hassan, G. Zaragoza, D.-C. Alarcón-Padilla. Steady state model for multi-effect distillation case study: Plataforma Solar de Almería MED pilot plant, Desalination, 37 (2014) 31–42.
[15] E. van de Ven, M.F.M. Speetjens, H. Weijdema, D.M.J. Smeulders, Modelling and further development of a multi-effect vacuum membrane distillation system, Aquaver & Technische Universiteit von Eindhoven (2014).
[16] C. Bidart, M. Fröhling, F. Schultmann, Municipal solid waste and production of substitute natural gas and electricity as energy alternatives, Appl. Thermal Eng., 51(1–2) (2013) 1107–1115.